Unidentified Particle Elliptic Flow in BRAHMS

Erik Johnson
University of Kansas
Last Modified: 1/6/06

This document is for BRAHMS internal use only.

The BRAHMS experiment has rearranged two rings of the silicon multiplicity array to be highly segmented in the ϕ direction. The rearrangement and the large event statistics of the Au-Au 2004 data run at RHIC allows BRAHMS to measure elliptic flow. The process of this measurement is outline is this paper, including a discussion on the systematic effects on the final results. With the results indicating that the array can be used for event plane correlations with the spectrometers, a discussion of the details involved in the measurement of the multiplicity array event plane is included.

Table of Contents:

page
Section 1: Data Set.....2
Section 2: Detector Geometry.....2
Section 3: Overview of Elliptic Flow.....2
Section 4: Measuring the Reaction Plane.....3
Section 5: Measuring the Reaction Plane Resolution Correction...10
Section 6: Background and Non-Flow Corrections.....13
Section 7: Measuring v_2.....14

Section 1: Data Set

The data set used in this note is from the Run04 AuAu events. I have tagged 411 valid runs ranging from 9389 to 10729.

Section 2: Detector Geometry

Two of the silicon rings were rearranged to allow for a more robust measure of the reaction plane. The elements used in this analysis is shown below.

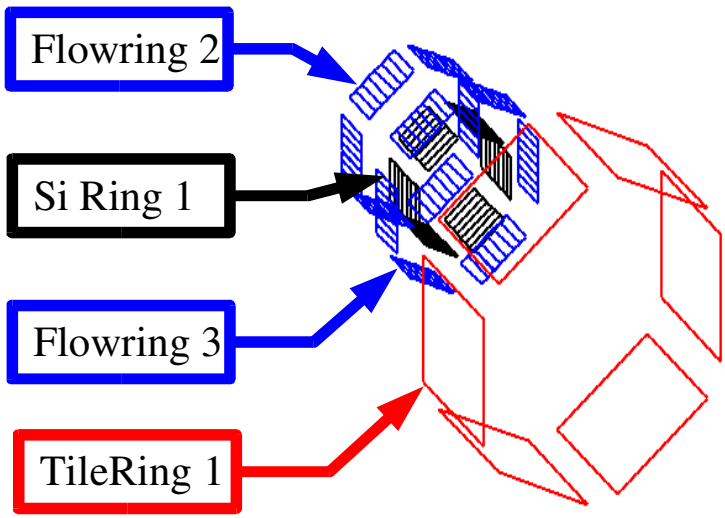

Figure 1Detector geometry of the four azimuthally symmetry rings used in the integrated flow analysis.

Section 3: Overview of Elliptic Flow

Azimuthally anisotropic flow is a result of the collision geometry of two colliding nuclei, time scales of the expansion, and pressure gradients in the collision region. Two nuclei that do not collide with an impact parameter of 0 carve out a collision region that has a shape similar to an American football. As a result of the non-central collision, pressure is built up higher in the reaction plane than out of plane. The reaction plane is defined by the impact parameter and the beam axis. The pressure gradients result in an azimuthally anisotropic distribution. This distribution is affected by the rate the spectator nucleon receded from the collision region. If the spectator nucleons do not recede from the collision region fast enough, the produced particles will rescatter with the spectator nucleons, and the region where the mean free path is largest is out of the reaction plane, thus giving an out of plane azimuthally anisotropic distribution. If the spectator nucleons recede fast enough, the distribution will tend toward an in-plane distribution. The time required for thermal freeze out also has an effect on the magnitude of the anisotropic flow signal. Large time scales result in decreasing the initial signal. In short, the azimuthally anisotropic flow signal is an initial state effect and is being well

represented by hydrodynamics.

Given a reaction plane, Ψ_R, the azimuthally anisotropic particle distribution can be represented by a Fourier expansion,

$$\frac{d^3N}{2\pi\, p_T dp_T dy d(\phi-\Psi_R)} = \frac{d^2N}{2\pi\, p_T dp_T dy}\left(1+\sum_n 2\, v_n \cos[n(\phi-\Psi_R)]\right) \quad (1)$$

The v_n terms are the magnitude of the flow signal in the n^{th} harmonic, and ϕ is the angle in azimuth of the particle. In the community, v_1 is termed the directed flow and v_2 is termed the elliptic flow. Each of the vn terms can be determined mathematically from

$$v_n = \langle \cos(n[\phi-\Psi_R])\rangle \quad (2)$$

Section 4: Measuring the Reaction Plane

The method described above requires that the reaction plane is known, but there is no direct method in measuring this plane. The method used to estimate the angle of the plane in ϕ is given by

$$\Psi_n = \frac{1}{n}\tan^{-1}\frac{\sum_i w_i \sin(n\phi_i)}{\sum_i w_i \cos(n\phi_i)} \quad (3)$$

where ϕ_i is the azimuthal angle of detector element i. w_i is a weight for each element based on the total energy deposited in that element.

$$w_i = energy_i \cdot NormW_i \quad (4)$$

where $energy_i$ is the total energy deposited in element i and $NormW_i$ is a normalization correction factor.

$$NormW_i = \frac{\sum_{events}\ \sum_{j=0-num\ ring\ elements} energy_j / Num\ of\ Ring\ Elements}{\sum_{events} energy_i} \quad (5)$$

In these sums, $energy_j$ is the energy in element j for the ring of element i. In short, the numerator is the average energy per element in a detector ring averaged over all events. The denominator is the average energy in element i over all events. The events used to generate these averages are the minimum bias events (trigger 4 & 5) for centralities from 0 to 40% and vertices from -36 cm to 36 cm.

The energy signal is used in this case because the total energy deposited over the η range studied here is relatively constant for a given centrality. This will remove any additional correction factors to the normalization weight that may depended any acceptance issues based on the vertex position.

It is important for flow end users to set up the mult rdo modules properly. Here one will have to specify that the energy to be saved to the outNode will be the total energy deposited, not the angle corrected energy deposited. Here are how the modules are setup for this analysis.

```
// ###################################################################
  fMinVtx  = -36;
  fMaxVtx = 36;
  fOffsetBB = 0;
  fOffsetINEL = 0;

  //_____________________________________________________________________
  // TMA Module
  BrTileRdoModule* tileModule = new BrTileRdoModule("Tile","Tile Reducer");
  tileModule->SetOutlierMethod(BrTileRdoModule::kNoCorrection);
  tileModule->SetMinVtx(fMinVtx);
  tileModule->SetMaxVtx(fMaxVtx);
  tileModule->SetOffsetBB(fOffsetBB);
  tileModule->SetOffsetINEL(fOffsetINEL);
  tileModule->SetSaveCorrectE(kFALSE);
  mainModule->AddModule(tileModule);

  //_____________________________________________________________________
  // SMA Module
  BrSiRdoModule* siModule = new BrSiRdoModule("Si","Si Reducer");
  siModule->SetOutlierMethod(BrSiRdoModule::kNoCorrection);
  siModule->SetMinVtx(fMinVtx);
  siModule->SetMaxVtx(fMaxVtx);
  siModule->SetOffsetBB(fOffsetBB);
  siModule->SetOffsetINEL(fOffsetINEL);
  siModule->SetSaveCorrectE(kFALSE);
  mainModule->AddModule(siModule);

  //_____________________________________________________________________
  // FlSi SMA Module
  BrFlSiRdoModule* flsiModule = new BrFlSiRdoModule("FlSi","FlSi Reducer");
  flsiModule->SetOutlierMethod(BrFlSiRdoModule::kNoCorrection);
  flsiModule->SetGeantResolution(1.0);
  flsiModule->SetMinVtx(fMinVtx);
  flsiModule->SetMaxVtx(fMaxVtx);
  flsiModule->SetOffsetBB(fOffsetBB);
  flsiModule->SetOffsetINEL(fOffsetINEL);
  flsiModule->SetSaveCorrectE(kFALSE);
  mainModule->AddModule(flsiModule);
  // ###################################################################
```

The results for only using the normalization weights are shown below. The reaction plane is determined for each ring: Tile1, Si1a,c-g, Flow2, Flow3, BBL4.

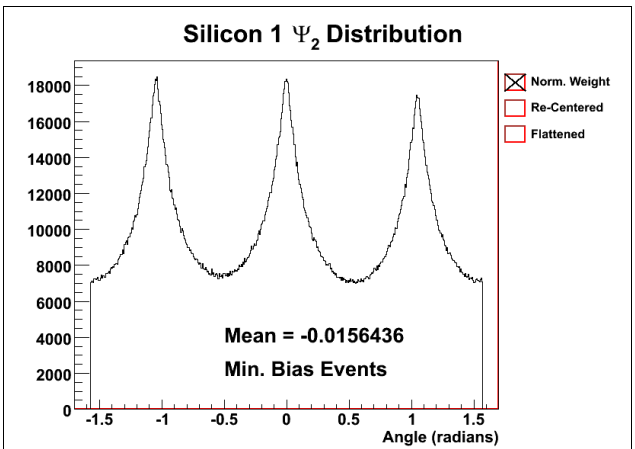

Figure 2

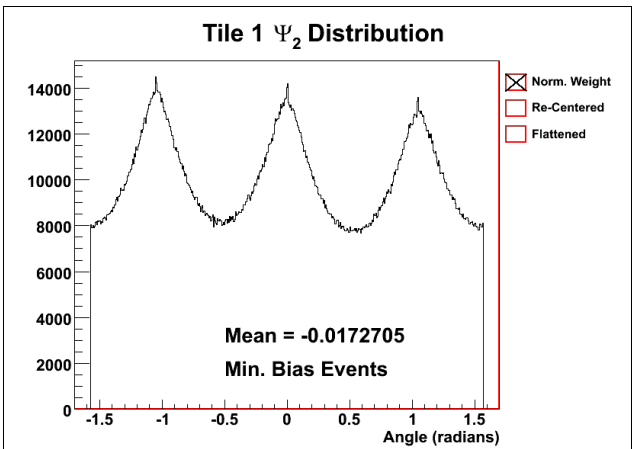

Figure 3

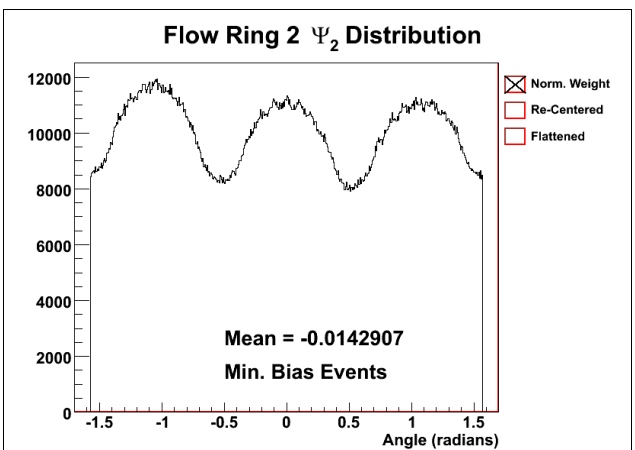

Figure 4

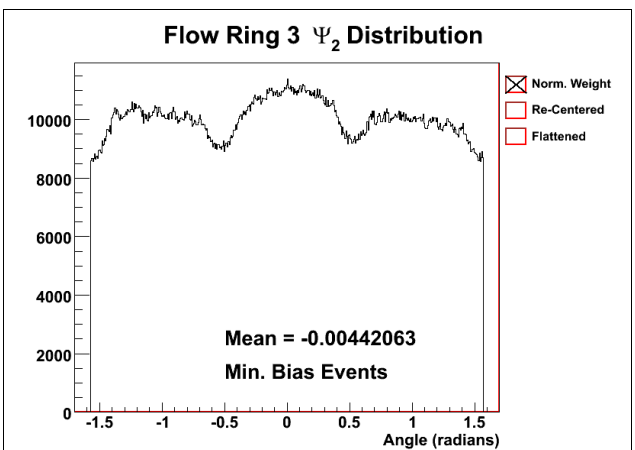

Figure 5

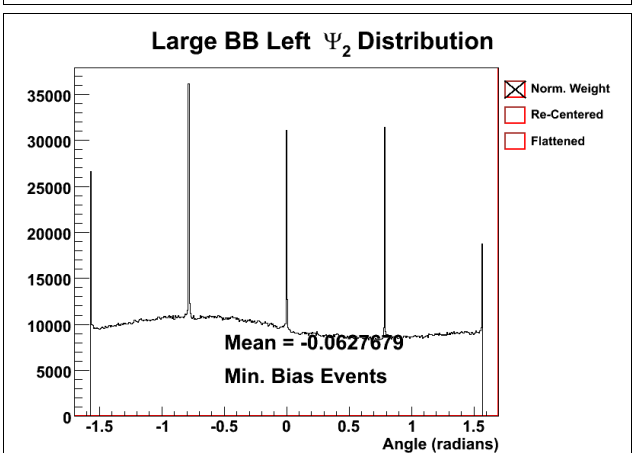

Figure 6

A combination reaction plane is determined using the silicon elements, which include the silicon rings a, c-g, flow ring 2, and flow ring 3. The reaction plane here is calculated using a slightly different method, which renormalizes the weights between each ring.

$$X_j = \sum_i w_{ji} \cos(2\phi_{ji}) \tag{6}$$

$$Y_j = \sum_i w_{ji} \sin(2\phi_{ji}) \tag{7}$$

here j represents ring j.

$$\Psi_n^{combo} = \frac{1}{n} \tan^{-1} \frac{\sum_j Y_j / \sqrt{X_j^2 + Y_j^2}}{\sum_j X_j / \sqrt{X_j^2 + Y_j^2}} \tag{8}$$

The resulting reaction plane looks like this.

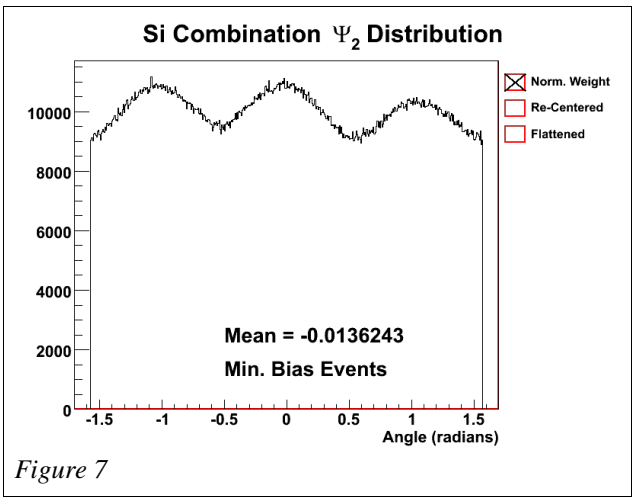

Figure 7

The first correction that is applied to the data is to recenter the x and y values, as shown in equations 6 and 7. These values over all events should be averaged to zero. But the data shows some slight offsets are are not accounted for in the normalization weights. Equations 6 and 7 now become

$$X_j = \sum_i w_{ji} \cos(2\phi_{ji}) - \langle \sum_i w_{ji} \cos(2\phi_{ji}) \rangle \tag{9}$$

$$Y_j = \sum_i w_{ji} \sin(2\phi_{ji}) - \langle \sum_i w_{ji} \sin(2\phi_{ji}) \rangle \tag{10}$$

Here the average is over all min. bias events. Remember that i stands for an element in ring j.
The resulting reaction planes are shown in the figures below. The averages were determined for a given centrality and eta bin. Only minimum biased events were used to generate these values.

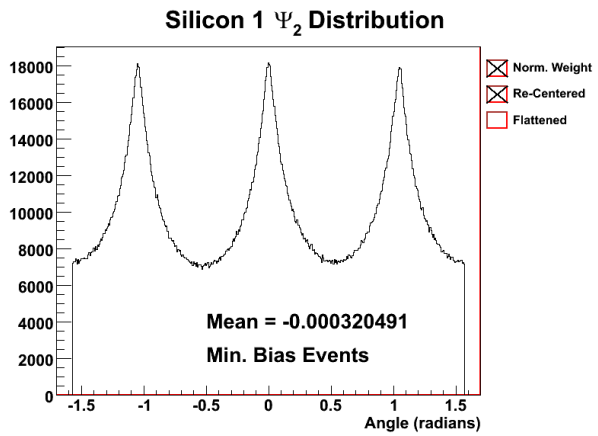

Figure 8

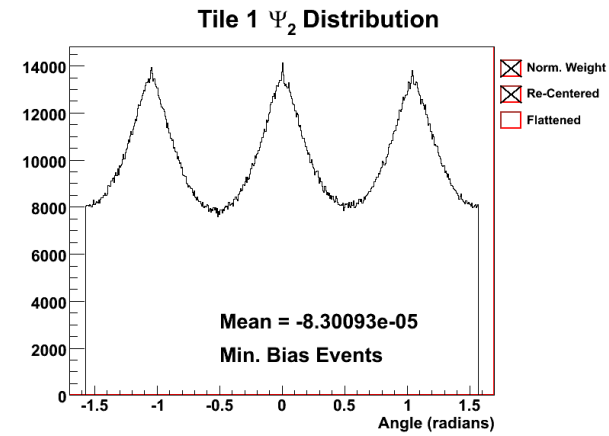

Figure 9

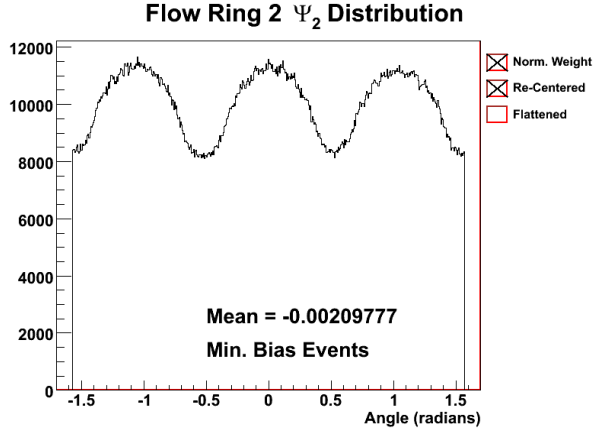

Figure 10

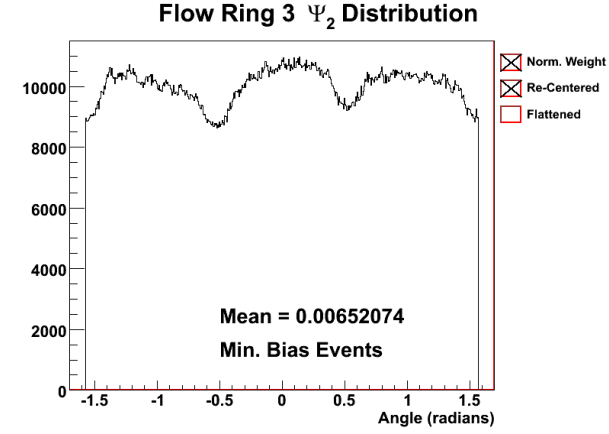

Figure 11

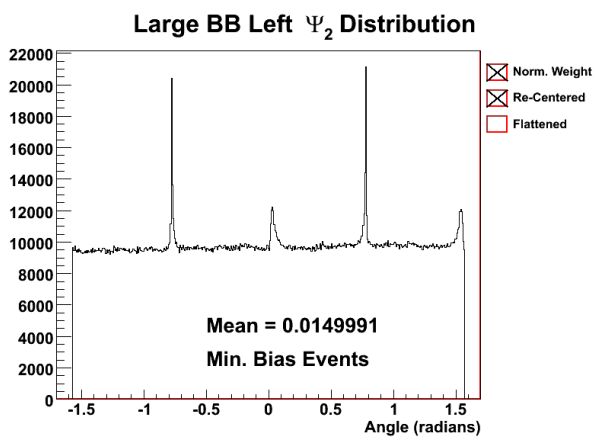

Figure 12

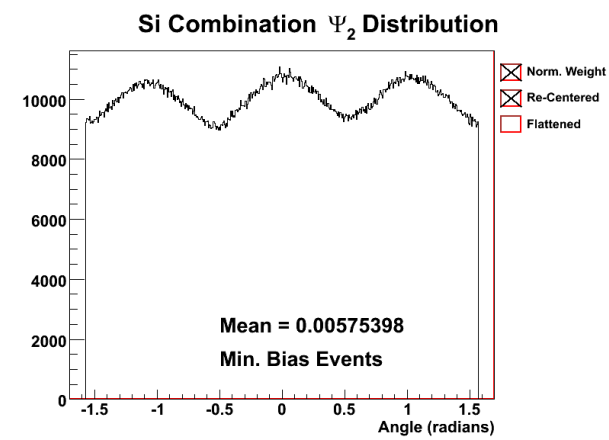

Figure 13

The last step in this process is to flatten the reaction plane. The idea behind this is to preserve the reaction plane resolution but to evenly distribute the reaction plane from -π/2 to π/2. This is done by making small adjustments to the distribution using a Fourier decomposition of the distribution. For a given reaction plane, Ψ, the flattened reaction plane is

$$\Psi^{flat} = \Psi + \sum_n \frac{2}{n+1}\{\langle \cos[(n+1)\Psi]\rangle \sin[(n+1)\Psi] - \langle \sin[(n+1)\Psi]\rangle \cos[(n+1)\Psi]\} \qquad (11)$$

the averages are determined for each ring and are over min. bias events for a given centrality bin. Also n was taken out to 20. For this analysis, it should be noted that this final correction is only applied to the reaction plane angle and not to the x and y values which are used to determine both the reaction plane and the v_2 signal. Only minimum biased events were used for this correction. The final reaction plane distributions are shown below.

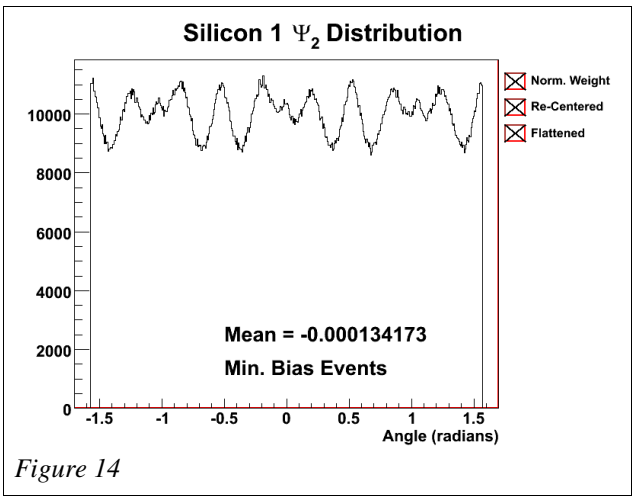

Figure 14

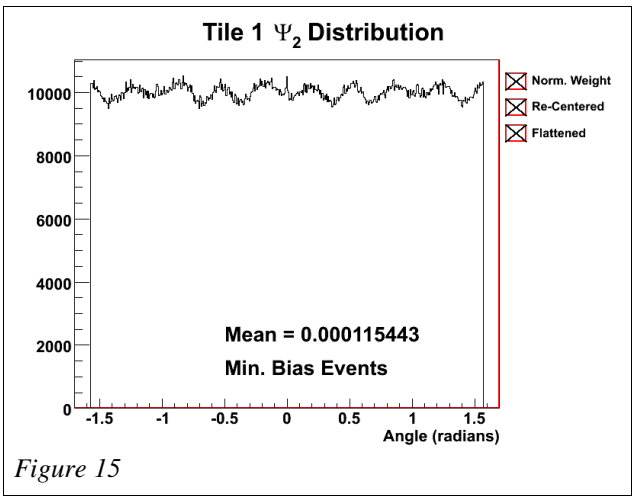

Figure 15

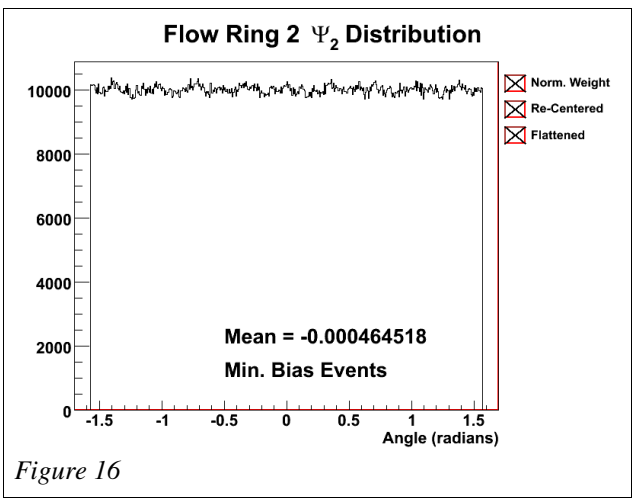

Figure 16

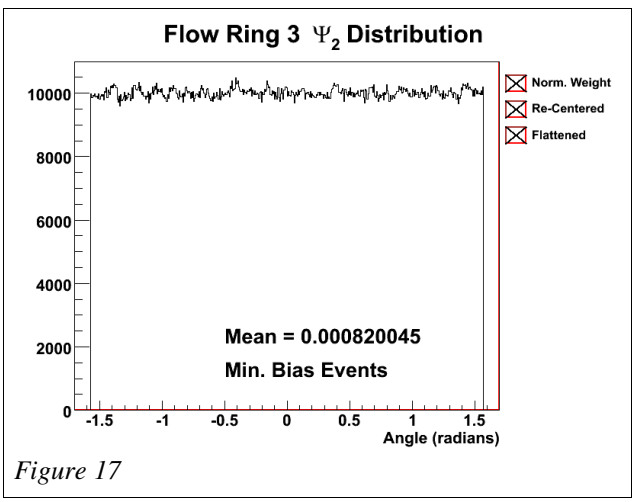

Figure 17

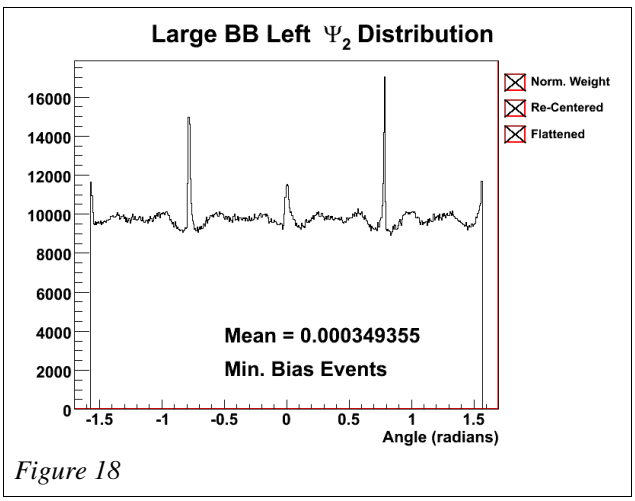

Figure 18

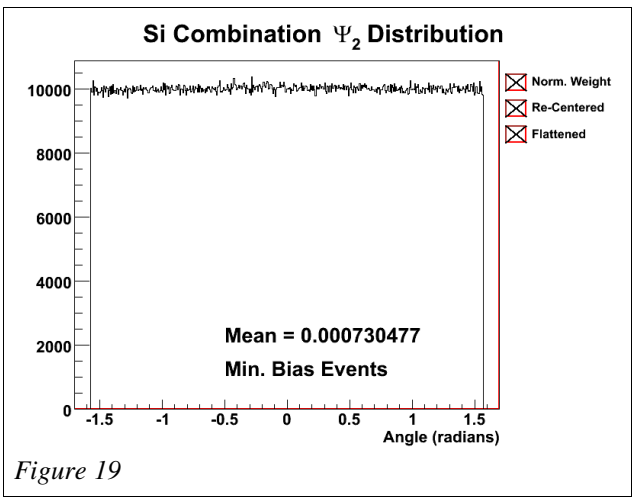

Figure 19

The spectrometer triggers affect the reaction plane distribution. This is best seen by looking at the silicon combination reaction plane for events. Here the corrections are only done for the min. bias events in order to not remove the effect. Figure 20 show a small bulge around an angle of zero. The spec. triggers are more efficient in selecting events where the reaction plane is horizontal because there is a non-zero v_2. The maximum effect is about 2% over min. bias events. The analysis using the spectrometer needs to suppress this effect, which can be done by using all events for the re-centering and flattening corrections. This analysis, where 2π detectors are used, this efficiency distortion must not be removed.

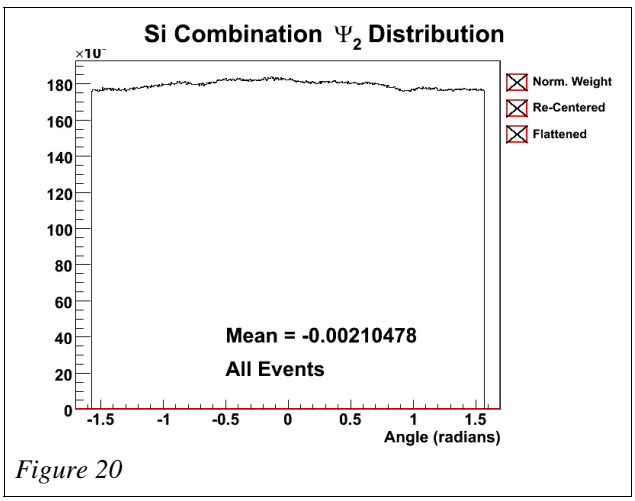

Figure 20

The combined reaction plane from all of the silicon rings is not used in this analysis and will not be discussed beyond this point. This has only been used here for illustrative purposes.

Section 5: Measuring the Reaction Plane Resolution Correction

The resolution correction factor is the inverse of the value discussed below, and in some literature the value is term the resolution. The value is used to correct for a suppression of the flow signal due to the inaccuracy of the measured reaction plane (ie. the resolution of the measured reaction plane).

The first step in measuring the correction value is to determine regions where two detectors do not over lap in eta. Any region where the detectors over lap will create an autocorrelation that will distort the measurement. Furthermore, the rings must be removed sufficiently away from each other to make sure that no backgrounds or secondaries produce any non-flow correlations between two detector rings. A band of 0.2 units in eta around each detector ring's acceptance has been used to ensure that the each ring measures completely independent particles. The last concern is that the vertex is not know to an infinite accuracy. The effective eta coverage of the detector rings is widened proportionally to the vertex resolution. For a vertex measured by the spectrometer, a vertex smear of 5mm is applied to the eta coverage, and for the BB vertex, the smear is 3cm. The resulting eta coverage for each ring is shown below.

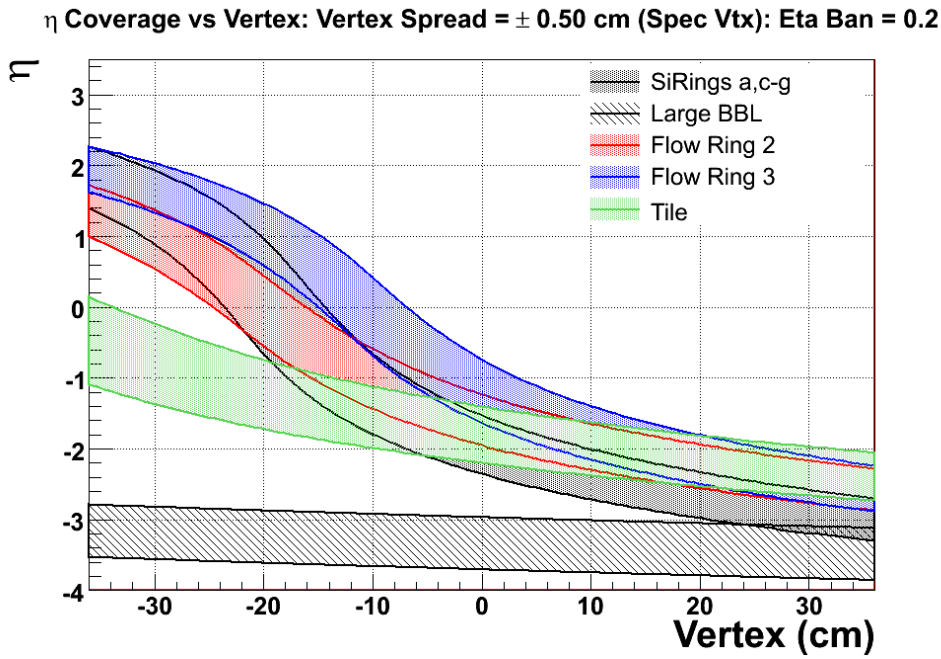

Figure 21

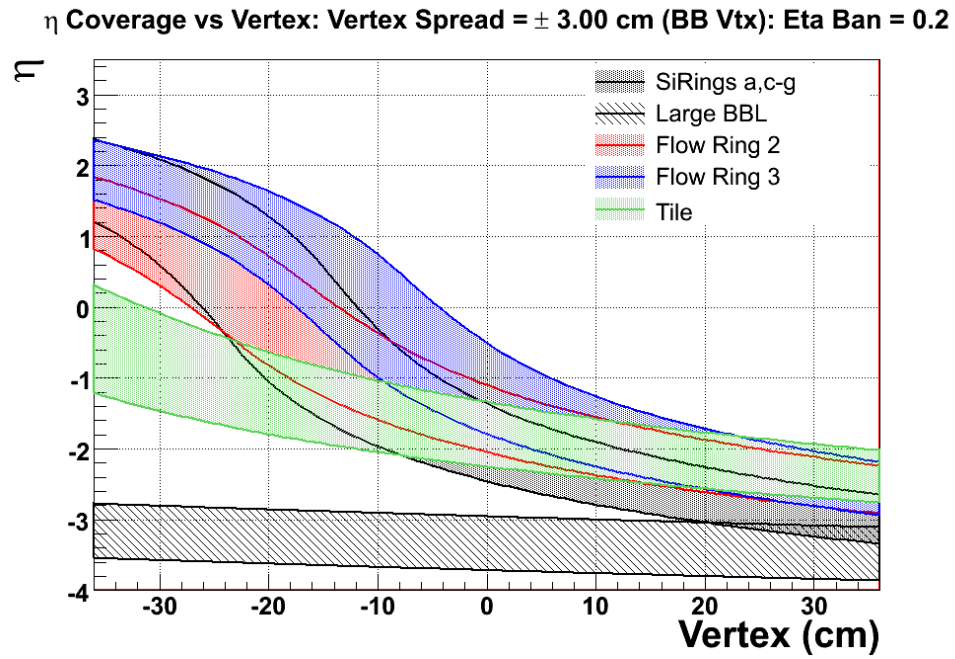

Figure 22

The standard method used to measure the resolution correction is to use the correlation between three measurements. This is given as

$$ResCor_a = \sqrt{\frac{\langle \cos[2(\Psi_a - \Psi_b)] \rangle \langle \cos[2(\Psi_a - \Psi_c)] \rangle}{\langle \cos[2(\Psi_b - \Psi_c)] \rangle}} \qquad (12)$$

a, b, and c are indices for three independent rings. The resolution correction for one ring can be determined by using various combinations between the five rings. The viable combinations where then averaged to give a final correction.

Figures 23 – 27 show the resolution correction for the centrality bin of 20% to 25% most central events. The resolution was determined for 9 centrality bins and 10 eta bins. These figures are shown to illustrate the shape of the reaction plane resolution and compare it to the resolution determined from a GEANT simulation. The input to the GEANT simulation is HIJING with default settings.

The resolution correction was applied on an event-by-event basis.

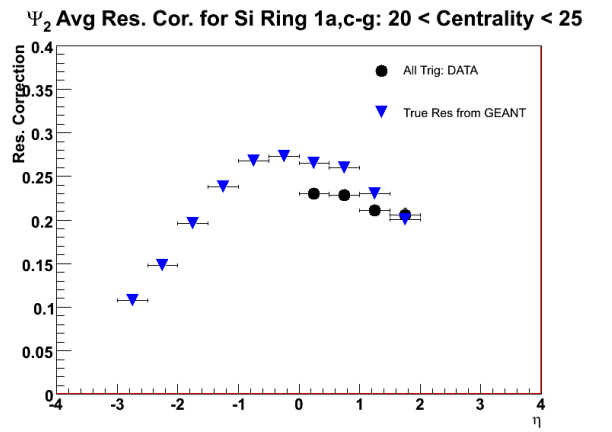

Figure 23

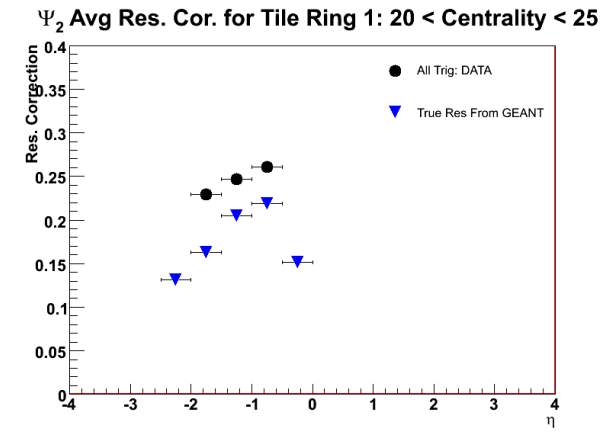

Figure 24

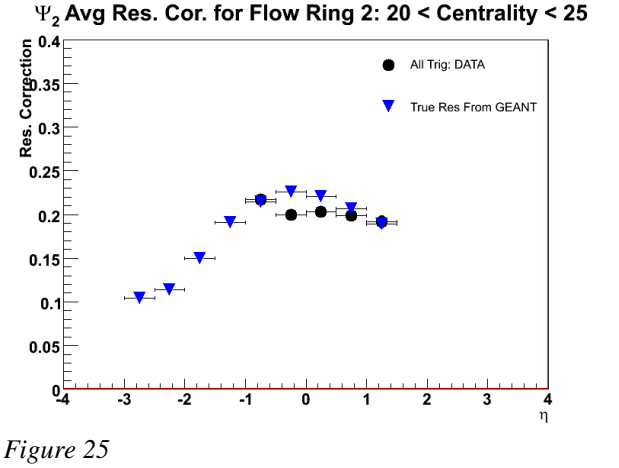

Figure 25

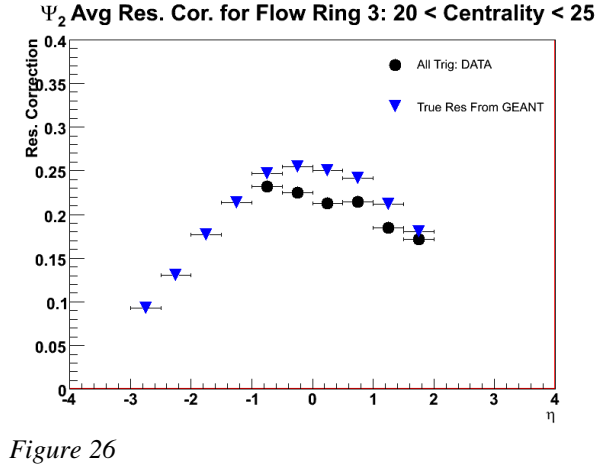

Figure 26

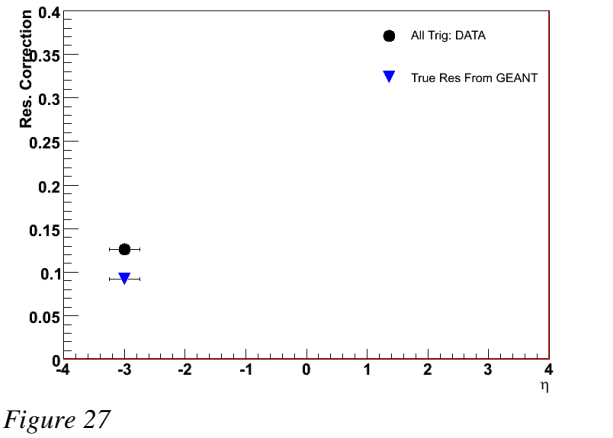

Figure 27

As one can clearly see, the resolution correction is similar to, but not exactly, the true reaction plane resolution determined from the GEANT simulation. This is most likely due to the differences between the HIJING multiplicity and the true multiplicity.

Section 6: Background and Non-flow Corrections

There are three effects that need to be corrected based on the GEANT simulations. These effects will be corrected with one scaling factor determined from taking the ratio of the input value of v_2 and the measured value of v_2.

The simulations have shown that there is a uniform background in ϕ, which suppresses the flow signal. Even though rings are only correlated when they are separated in h by at least 0.2 units (see figures 21 and 22), there is a chance that a secondary produced in one ring can be incident on another. This effect will enhance the flow signal and needs to be removed. The final effect is due to the geometry of detector rings. The tile and silicon rings with six elements have a large acceptance in ϕ per element. When the calculations are made, the total signal in that element is given one ϕ position. In effect, the resulting flow signal will be suppressed.

The HIJING code was changed such that a flow signal can be induced on the particles. Two elliptic flow signals were used. One was a parameterization of the Phobos data and the other was a constant 5% elliptic flow. The elliptic flow measured using the true reaction plane is used because the resolution correction discussed in section 5 accounts for these affects on the reaction plane. Figure 28 shows the correction factor determined from the Phobos input and the 5% input. The different colors represent a different detector ring, and within a color scheme, the shapes are separate rings. For this note, the only point from the plot is that the corrections are similar. The greatest deviations are at the highest eta where the signal is the smallest and will have the least affect. To ensure that the correction isn't being used to mimic the Phobos data, the 5% values were used to given the final elliptic flow measurement. Finally, it is believed that these corrections will be independent of centrality, and therefore, the values shown in figure 28 are for the 0-70% central events.

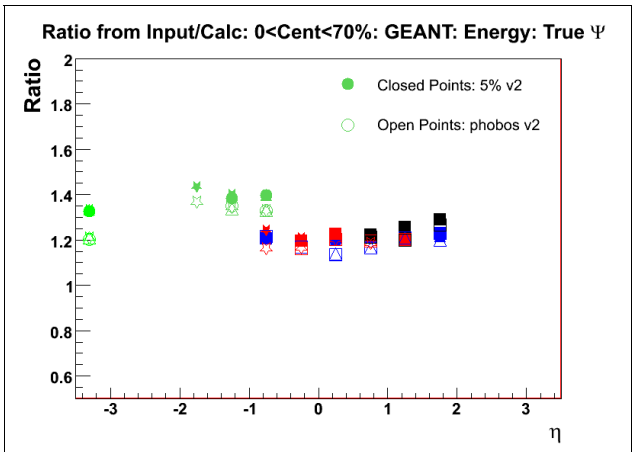

Figure 28

Section 7: Measuring v_2

Up to this point it has been mentioned that the data has been divided into various bins of centrality and eta. Here are the bins that have been used.

Centrality Bins

Bin	***0***	***1***	***2***	***3***	***4***	***5***	***6***	***7***	***8***
Min	0%	5%	10%	15%	20%	25%	30%	40%	50%
Max	5%	10%	15%	20%	25%	30%	40%	50%	70%

Eta Bins

Bin	***0***	***1***	***2***	***3***	***4***	***5***	***6***	***7***	***8***	***9***
Min	-3.0	-2.5	-2.0	-1.5	-1.0	-0.5	0.0	0.5	1.0	1.5
Max	-2.5	-2.0	-1.5	-1.0	-0.5	0.0	0.5	1.0	1.5	2.0

The data is stored in a tree that holds the X and Y values from equations 6 and 7 for each ring. The data needs to be corrected using the methods explained above on an event-by-event basis. The X and Y values are re-centered (see equations 9 and 10), and then the reaction planes for each ring are flattened (equation 11). Here we will defined the re-centered X and Y values as Qx and Qy, and the flattened reaction plane as Ψ^{flat}. The observed v_2 signal is done by using the average shown below over all particles in all events for a given eta and centrality bin

$$\langle \cos[2(\phi_a - \Psi_b^{flat})] \rangle = v_2^{obs} = \frac{\sum_{event\ e} \cos(2\Psi_{be}^{flat}) \cdot Qx + \sin(2\Psi_{be}^{flat}) \cdot Qy}{\sum_{event\ e} \sum_{element\ i} w_{ie}} \qquad (16)$$

Here the denominator is just the total sum of all the normalized weights from equation 4 over all the elements in ring a and over all the events. The resolution effect is also corrected on the fly, meaning that the correction is applied while these sums are being tallied. Equation 16 now becomes

$$v'_2 = \frac{\sum_{event\ e} \{\cos(2\Psi_{be}^{flat}) \cdot Qx + \sin(2\Psi_{be}^{flat}) \cdot Qy\} / ResCor_{be}}{\sum_{event\ e} \sum_{element\ i} w_{ie}} \qquad (17)$$

After the sums have been tallied the final correction for the background and non-flow corrections are applied for the various eta bins, not centralities. The factors are just the ratios between the input of 5% v_2 and measured values from GEANT simulations for 0-70% centralities.

A comparison with the Phobos data in eta for the 15% to 25% central events is shown in figure 29. The centrality dependence is shown in figure 30. As shown, the BRAHMS integrated v_2 is in good agreement with the Phobos v_2 signal.

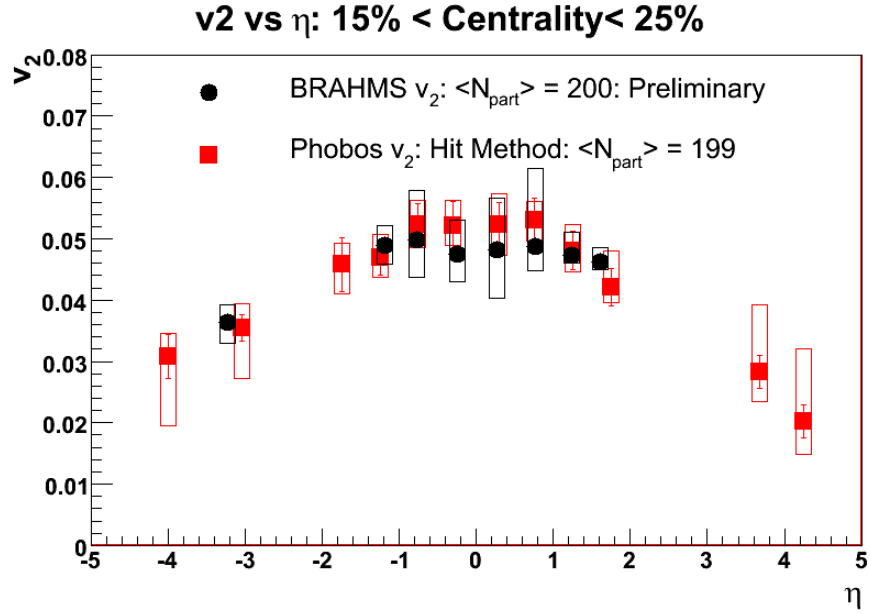

Figure 29

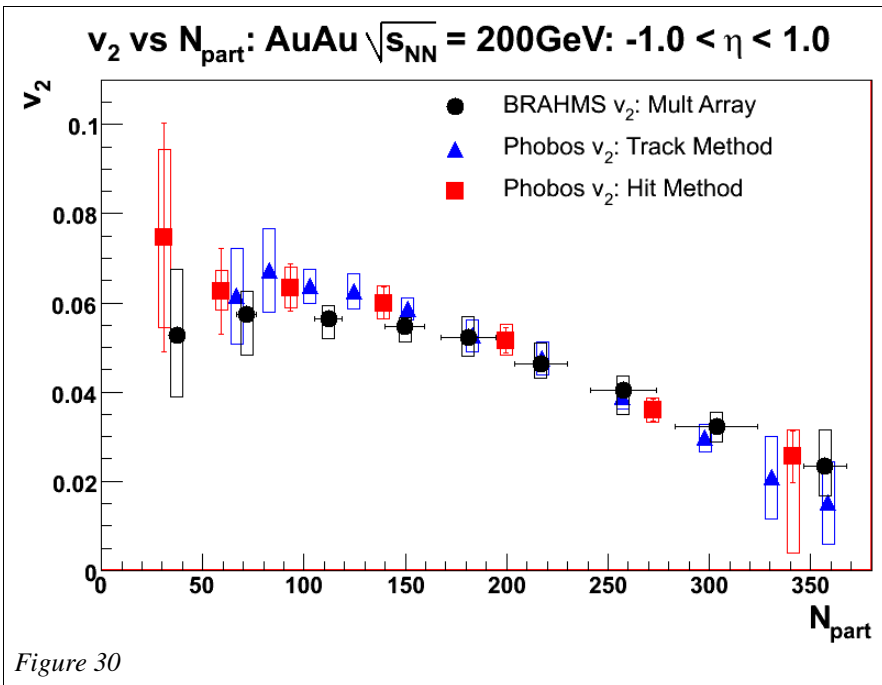

Figure 30